

S. SENTHILARASU¹
S. VELUMANI^{2,✉}
R. SATHYAMOORTHY¹
A. SUBBARAYAN¹
J.A. ASCENCIO²
G. CANIZAL²
P.J. SEBASTIAN^{2,3}
J.A. CHAVEZ⁴
R. PEREZ²

Characterization of zinc phthalocyanine (ZnPc) for photovoltaic applications

¹ R & D Department of Physics, Kongunadu Arts and Science College, Coimbatore-641029, India

² Programa de Investigación y Desarrollo de Ductos, Instituto Mexicano del Petróleo, Eje Central Lázaro Cárdenas, C.P. 07730, México D.F., México

³ CIE-Universidad Nacional Autónoma de México, Temixco, Morelos 62580, México

⁴ IIM, Universidad Autónoma de México, Circuito Exterior, C.U., C.P. 04510, México D.F., México

Received: 21 March 2003 / Accepted: 24 March 2003
Published online: 5 June 2003 • © Springer-Verlag 2003

ABSTRACT Zinc phthalocyanine (ZnPc) is a promising candidate for solar-cell applications, because it is easily synthesized and is non-toxic to the environment. Recently, phthalocyanine (Pc) was considered by many researchers as the active part in all-organic solar cells, i.e. plastic solar cells. It is a self-assembling liquid crystal developed from a common deep-blue-green pigment. It exhibits a characteristic structural self-organization, which is reflected in an efficient energy migration in the form of extinction transport. In this paper we have report structural, surface morphological, optical and thermal properties of flash-evaporated zinc phthalocyanine thin films. The samples were prepared by using a vacuum coating unit on well-cleaned glass substrates under a pressure of 7×10^{-6} Torr. A constant rate of evaporation (1 \AA/s) was maintained throughout the evaporation of the ZnPc thin films. A rotary drive was employed to obtain uniform thickness during the evaporation. Thicknesses of the films were monitored by a quartz-crystal thickness monitor and were cross verified by the multiple-beam interferometry technique. The X-ray-diffraction pattern reveals the crystalline nature of the films deposited at higher substrate temperatures. Scanning electron microscope and scanning probe microscope nanoscope studies were carried out to determine the surface uniformity and homogeneity of the films for interfacing and application purposes. All the films were found to possess small crystallites less than 100 nm in size. The optical transmittance measurements were carried out using a spectrophotometer in the visible region (400–800 nm) and the films were found to be absorbing in nature. The band gap of the ZnPc thin films is 1.97 eV and the optical transition was found to be direct and allowed. The absorption coefficient, extinction coefficient and refractive index of the ZnPc films were evaluated and the results are discussed. Differential scanning calorimetry studies of ZnPc films were carried out and a phase transition from α to β was observed at 538 K.

PACS 78.20.-e; 65.90.+i; 61.16.Ch; 61.16.Bg

1 Introduction

Photovoltaic cells fabricated with organic semiconductors have attracted considerable attention because of

their flexibility in varying their electrical and optical properties, and in general they can be more easily fabricated than any inorganic photovoltaic cells. Also organic semiconductors are promising materials for other optoelectronic applications such as light-emitting diodes (LEDs) and optical switches [1]. Phthalocyanine (Pc) is a well-known organic semiconductor and is suitable for use in photovoltaic devices since its physical and chemical durability is very high. A number of studies of functional properties of organic semiconductors have recently been carried out concerning both basic and application aspects. Phthalocyanines are one group of such materials, of which optical, electronic and photoelectronic properties are being extensively investigated [2]. Many kinds of phthalocyanines, such as metal-free phthalocyanines and phthalocyanines with various metals have been synthesized and are now utilized in a wide variety of fields like solar cells [3, 4], clinical photodynamic therapy [5], etc. Among these zinc phthalocyanine (ZnPc) ($C_{32}H_{16}N_8Zn$) is a promising organic semiconductor for photovoltaic applications. The major part of the incident light in the visible region is absorbed and effectively contributes to photocarrier generation and the excited carriers play an important role in the photovoltaic effect. Even though a lot of research has been pursued on various phthalocyanines, to the knowledge of the authors and from the available literature not much work has been carried out on basic studies of zinc phthalocyanine thin films, and more detailed investigations are needed before going in for an all-organic solar cell. Hence, in this paper we present our partial work made on the fundamental characterizations like structural, surface analysis, optical and thermal properties of flash-evaporated zinc phthalocyanine thin films.

2 Experimental details

2.1 Flash evaporation

Flash evaporation is one of the easiest and most flexible techniques for the deposition of thin films. The objective of film-composition control is well accomplished by evaporating to completion even small quantities of the constituents in the desired ratio. Figure 1 shows the flash-evaporation setup. In the present setup only one filament was used at a temperature sufficiently high to evaporate the less volatile material. Although fractionation occurs during the

✉ Fax: +52-55/3003-6429, E-mail: velu@imp.mx

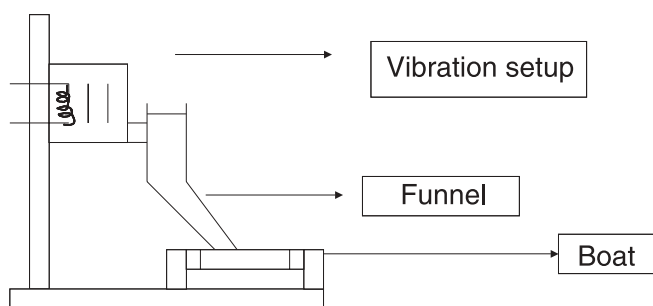


FIGURE 1 Flash-evaporation setup

evaporation of each particle, the latter are so small that stratification in the film is limited to a few atomic layers. These potential inhomogeneities are further reduced by dispensing the evaporant in a steady trickle, so that there are several different particles at all times. Hence, maintaining the uniform composition of that of the source material and accordingly excellent control of the film composition can be achieved by this method of film preparation.

Zinc phthalocyanine (Fluka Chemie, 98%) in bulk form was purchased and used without further purification. Zinc phthalocyanine layers of different thicknesses (28 Å to 168 Å) were deposited on well-cleaned glass substrates by the flash-evaporation technique under a starting pressure of 6×10^{-6} Torr. Flash evaporation has mostly been performed in a vacuum of 10^{-5} to 10^{-4} Torr. This is attributable to the high gas content of the evaporant powder and outgassing from the surfaces surrounding the relatively large flash-filament area. The thickness was determined by a quartz-crystal oscillation monitor and is cross verified by the multiple-beam interferometer (MBI) technique. Structural characterizations of the films were carried out using a JEOL model JDX8030 X-ray diffractometer. Scanning electron microscopy (SEM) analyses were done using a LEICA-CAMBRIDGE Stereoscan 440 and atomic force microscopy (AFM) analyses were performed using a multi-mode scanning probe microscope (SPM) (Nanoscope IV, Digital Instruments). The transmittance and absorbance spectra were recorded in the wavelength range 400–900 nm using a JASCO V-570 spectrophotometer. The phase-transition temperature was determined using a Perkin-Elmer DSC-7 differential scanning calorimeter.

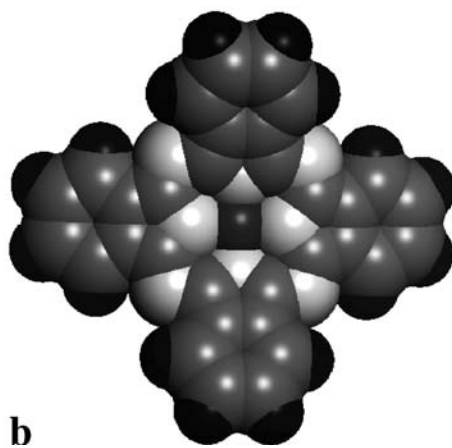
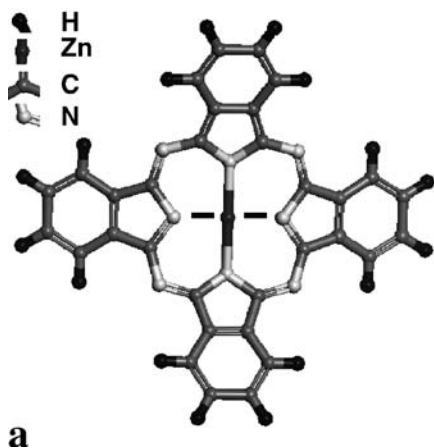


FIGURE 3 Molecular structure of the ZnPc used for flash evaporation. **a** Stick display and **b** atomic radius representation for minimum-energy configuration

3 Results and discussion

3.1 Structural studies

The structural analysis for the bulk as well as the films was carried out by the X-ray-diffraction (XRD) technique. Figure 2 shows the XRD pattern for the bulk zinc phthalocyanine powder and Fig. 3 shows the corresponding molecular model of bulk ZnPc; the latter figure shows a stick display in order to identify the structural nomenclature (Fig. 3a) and an atomic radius representation (Fig. 3b) that allows us to understand the elemental interaction at minimum-energy configuration (calculated by a density functional theory method). The XRD pattern exhibits a crystalline nature; the different major diffraction peaks are indexed and the values of interplanar spacing d are evaluated and compared with the standard data from JCPDS-ICDD tables for monoclinic ZnPc. Table 1 shows a comparative look at the calculated and standard d values for corresponding diffraction angles. Almost all the peaks corresponding to monoclinic ZnPc structure were obtained. Figure 4a and b show the XRD patterns of the flash-evaporated ZnPc films and the films are found to be dark blue in color with good adhesion over the substrate. The films deposited at room temperature ($T_s = 303$ K) are found to be amorphous in nature as shown in Fig. 4a and the films deposited at a higher substrate temperature ($T_s = 373$ K) are found to be polycrystalline in nature from the presence of many peaks (Fig. 4b). The diffraction-peak positions were compared with the standard JCPDS-ICDD tables and found to coincide well for monoclinic ZnPc structure. The diffraction line at $2\theta = 6.8^\circ$ in the XRD pattern corresponds to 1.29-nm spacing. Uyeda et al. [2, 6] and Debe et al. [7] suggested that the crystal structure of vacuum-evaporated ZnPc films is mon-

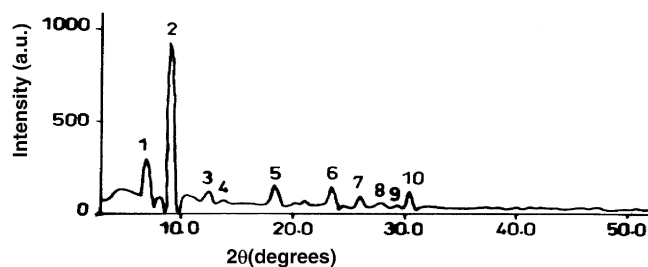


FIGURE 2 XRD pattern of the bulk ZnPc powder

Standard values			Experimental values		
2θ	d	I	2θ	D	I
6.800	12.988	303	6.977	12.658	100
9.100	9.710	926	9.278	9.524	90
12.500	7.075	121	12.559	7.042	20
13.800	6.412	76	14.070	6.289	5
18.500	4.792	144	18.707	4.739	30
23.500	3.783	150	23.647	3.759	50
26.000	3.424	98	25.815	3.448	20
27.800	3.206	63	27.994	3.185	25
29.300	3.046	45	29.543	3.021	5
30.400	2.938	127	30.548	2.924	30

TABLE 1 Comparison of calculated and standard XRD peaks and d values for bulk ZnPc powder

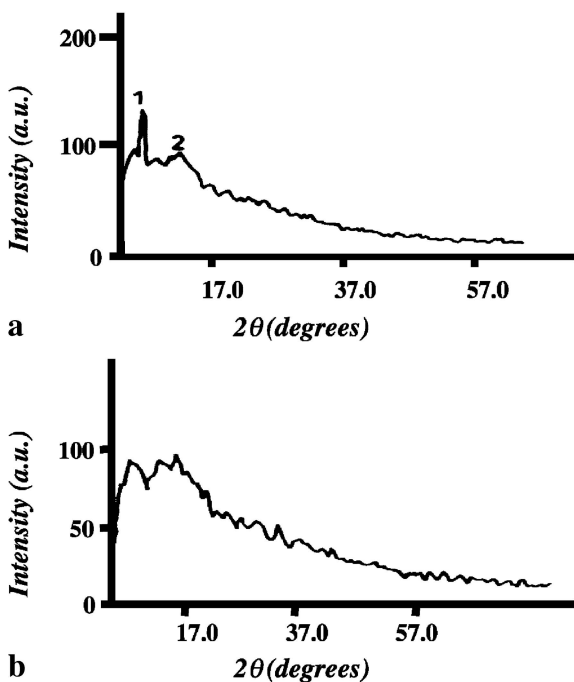


FIGURE 4 XRD pattern of the flash-evaporated ZnPc film at a substrate temperature of **a** $T_s = 303$ K and **b** $T_s = 373$ K

oclinic and the 1.3-nm spacing of (200) planes in α -ZnPc. Hence the spacing of the lattice planes of the crystallites is parallel to the surface of the ZnPc layer and these interpretations are in good agreement with our results.

3.2 Surface morphological studies

For device applications and to form junctions with various materials, an in detail analysis of the surface is needed; hence SEM and AFM analysis were carried out on crystalline samples. The surface morphology of a typical flash-evaporated ZnPc film deposited at $T_s = 373$ K is shown in Fig. 5. From the surface analysis, the films are found to possess a uniform thickness distribution. The SEM micrograph indicates a smooth surface with a crystalline nature of the deposited films and the crystallites are found to be small, less than 100 nm, contributing to broad peaks in the XRD pattern.

In order to analyze the surface characteristics in more detail, sampling methods of AFM were used, and the contact mode was applied. Figure 6a shows a three-dimensional rep-

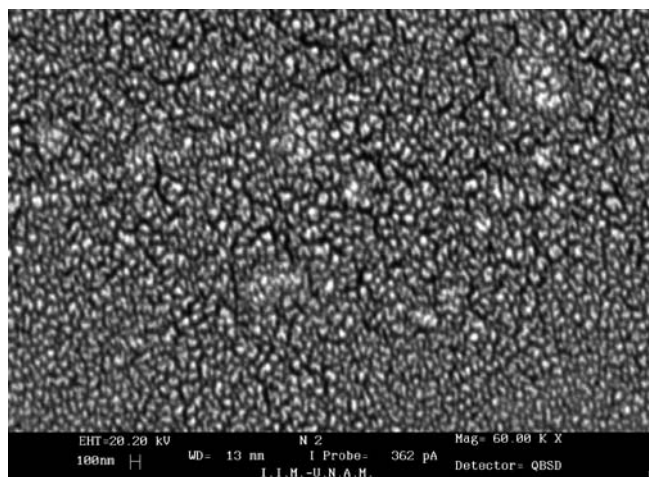


FIGURE 5 SEM micrograph of a flash-evaporated ZnPc film deposited at a substrate temperature of $T_s = 373$ K

resentation of the image obtained from the surface of flash-evaporated ZnPc films. A homogeneous distribution of crystalline domains can be observed from the image. From the sectional analysis of the films at various points, the topography is also very regular with variations of less than 20 nm as shown in Fig. 6b, which corresponds to different sections from the image. The size distribution is shown in Fig. 6c, which was obtained from several analyses for more than 300 crystalline domains. In the size-distribution plot, it is clear that there is a tendency to form domains of more than 50 nm and the main distribution is around 90 nm, which is well revealed from the SEM analysis also (Fig. 5). The deflection image of the ZnPc surface is shown in Fig. 7a, from which the crystallite distribution was observed to be uniform and regular. From the comparison of the deflection image (Fig. 7a) and the altitude topography (Fig. 6a) it is observed that the crystallite domains were of the same size.

With help of the deflection signals from the piezoelectric sensor of the SPM, the differences in composition or structure on the surface of a sample can be studied from the effects on the mechanical phase over the tip of the microscope. We obtained the information from the sample surface, which is shown in Fig. 7a, where the effect of homogeneity is proportional to the altitude information. Figure 7b shows the profile analysis of the surface image, that is, a plot between the changes in the potential measured versus the distance at various points on the surface of the ZnPc film. The change in potential measured from the piezoelectric sensor is directly proportional to the magnitude of the change in the homogeneity of the film, which in turn indicates the stoichiometry of the film. In our case the change in the potential was observed to be very low and the peaks are in the order of 0.04 V. This implies that there is a homogeneous distribution of the particles during the deposition and there is not much dissociation of the compound due to the flash evaporation.

3.3 Thermal analysis

In phase-equilibrium determination, thermal methods of analysis are used to detect phase transitions. A change in phase involves structural changes in the material

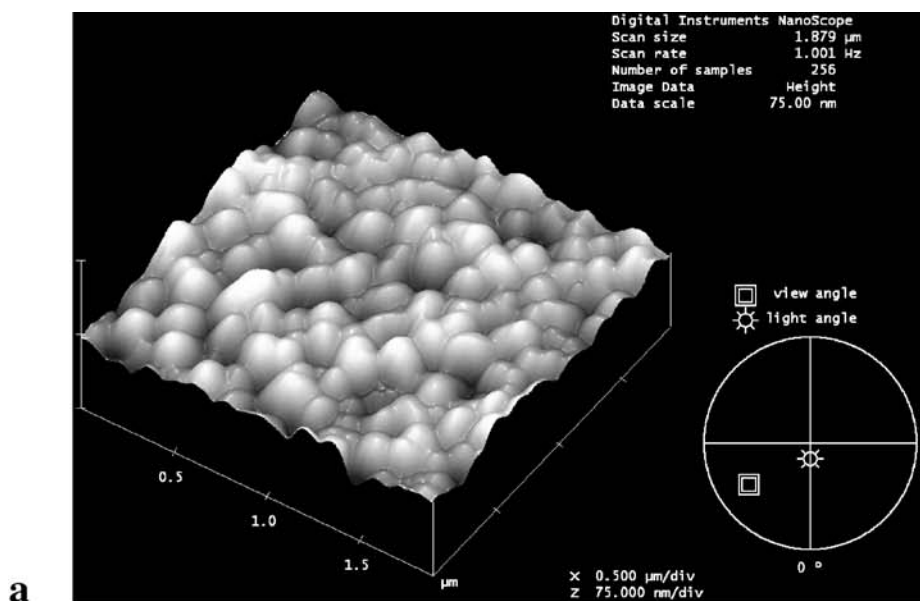
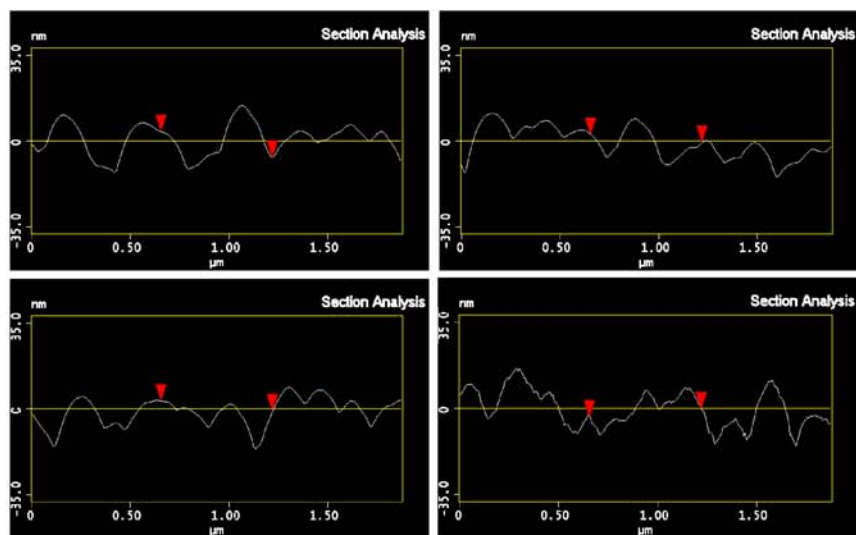
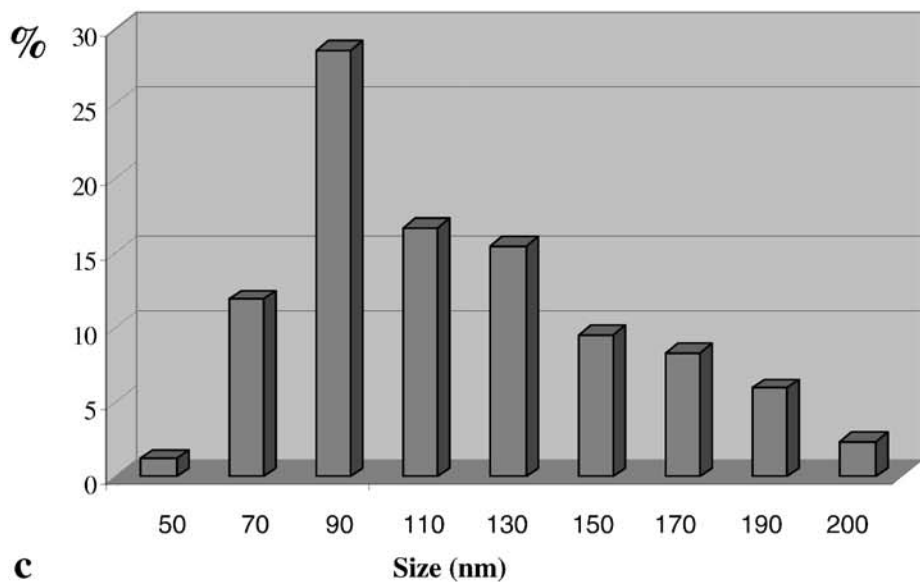
**a****b****c**

FIGURE 6 Three-dimensional SPM nano-scope analysis of the surface of flash-evaporated ZnPc film deposited at a substrate temperature of $T_s = 373$ K. **a** Three-dimensional image, **b** sectional analysis indicating the size distribution and **c** size-distribution plot

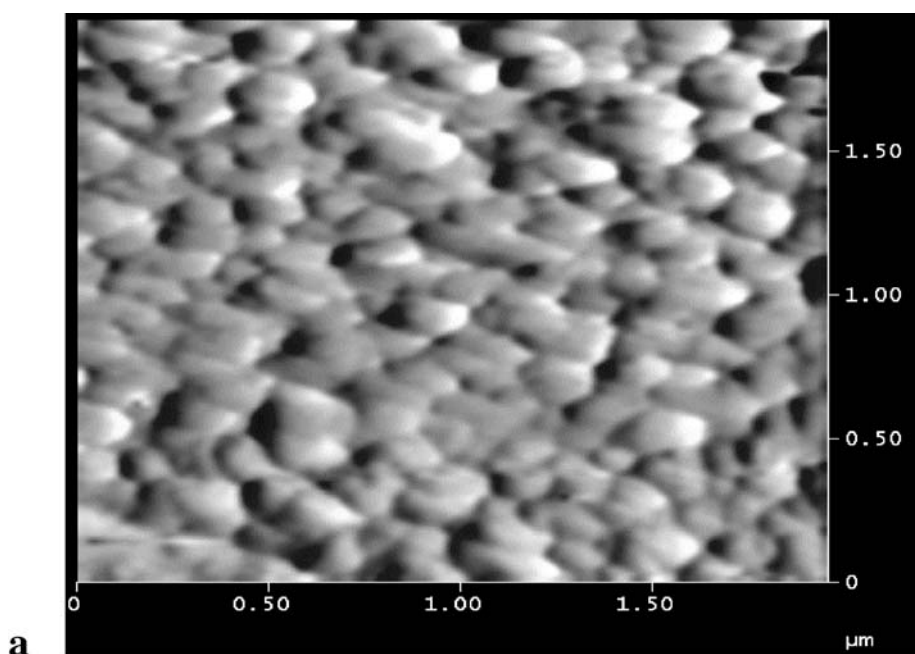
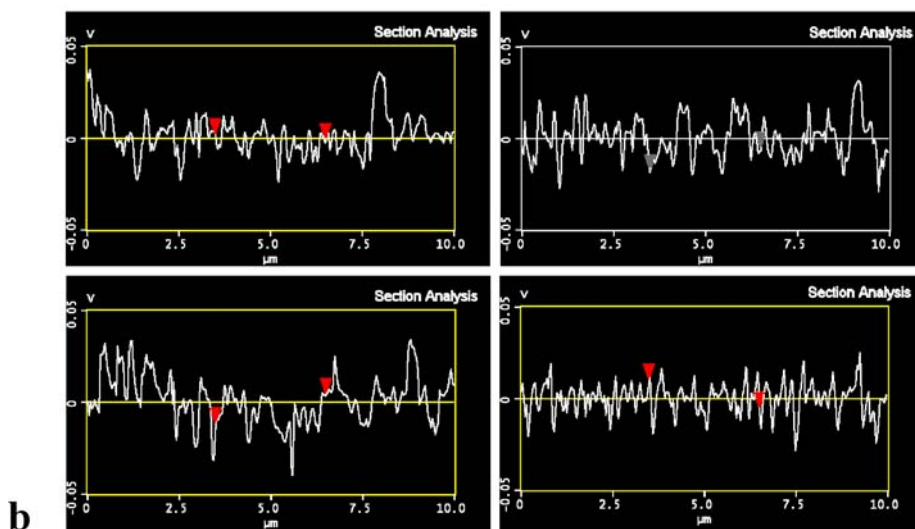


FIGURE 7 Surface analysis of the flash-evaporated ZnPc films from the SPM nanoscope in deflection mode. **a** Deflection-mode image and **b** plot of potential developed at various sections related to composition and structural changes



that are accompanied by evolution or absorption of heat. Thus, if a specimen is heated or cooled under uniform conditions, a structural change will be indicated by a temperature peak. The phase-transition temperature was measured by a differential scanning calorimeter, a Perkin-Elmer model DSC 7. The powder specimen scratched from thin-film samples of 11.8 mg was set in an aluminium crucible with a diameter of 9 mm and a height of 6 mm. The heating rate (dT/dt) was $10^{\circ}\text{C}/\text{min}$. Figure 8 shows the phase-change curve for a typical ZnPc thin-film sample deposited at 303 K. The peak is at 538 K, but the energy released by the sample starts at 505 K and ends at 553 K. Hence at 538 K the film changes its phase from α phase to β phase.

3.4 Optical properties

Analysis of the optical transmittance/absorption spectra is one of the most productive tools for understand-

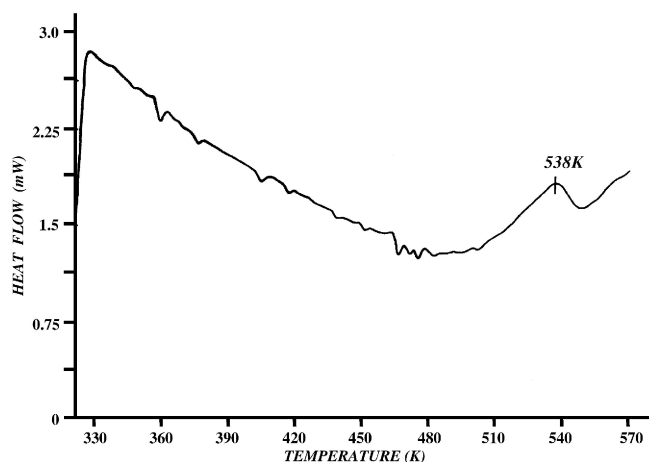


FIGURE 8 Phase-change curve for a typical flash-evaporated ZnPc thin film

ing and developing the band structure and energy gap of both crystalline and amorphous systems. The optical transmittance, reflectance and absorbance spectra of the ZnPc thin films were recorded by a Jasco V570 spectrophotometer. Figure 9 shows a typical absorbance spectrum of the flash-evaporated ZnPc films on glass substrates. The transmittance spectra of ZnPc films of different thicknesses reveal that the transmittance decreases with the increase of the film thickness. Normally, organic molecules of phthalocyanine and their derivatives exhibit anomalous optical characteristics because of their unique molecular ring structures. It is well known that they possess two kinds of energy bands. In the case of phthalocyanines, one of them is called the *Q* band, which is equivalent to the α band in porphyrins, and the other one is called the *B* band, which is equivalent to the γ or Soret band in porphyrins [8]. The origins of the *Q* band and the *B* band are an a_{1u} to e_g transition, and an a_{2u} to e_g and a b_{2u} to e_g transition, respectively [6]. The peak wavelengths in the absorption spectrum are found at 330 nm and 690 nm and the wavelengths of the shoulders are around 305 nm and 730 nm. The absorption peak at 690 nm corresponds to the *Q* band, whereas 330 nm corresponds to the *B* band [9]. From the transmittance values, the refractive index (*n*) and extinction coefficient (*k*) were calculated using (1) and (2) below by the iterative method.

$$T = \frac{n_2}{n_0} \frac{e^{2\alpha l} + (g_1^2 + h_1^2)(g_2^2 + h_2^2)(e^{-2\alpha l} + C \cos 2r_1 + D \sin 2r_1)}{e^{2\alpha l} + (g_1^2 + h_1^2)(g_2^2 + h_2^2)(e^{-2\alpha l} + C \cos 2r_1 + D \sin 2r_1)} \quad (1)$$

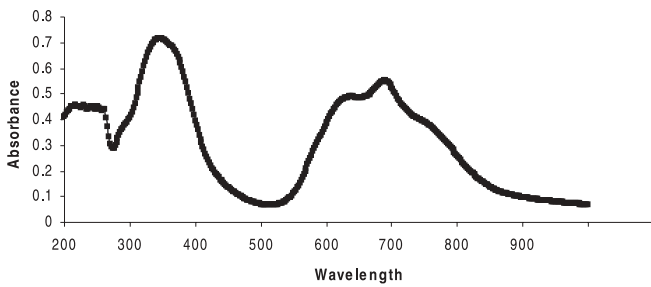


FIGURE 9 Absorption spectra for a typical flash-evaporated ZnPc thin film

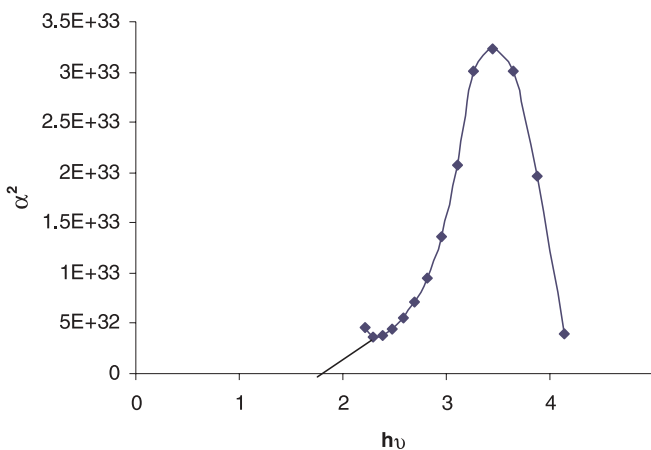


FIGURE 10 α^2 versus photon-energy curve for a typical flash-evaporated ZnPc thin film

$$R = \frac{(g_1^2 + h_1^2) e^{2\alpha l} + (g_2^2 + h_2^2) (e^{-2\alpha l} + A \cos 2r_1 + B \sin 2r_1)}{e^{2\alpha l} + (g_1^2 + h_1^2) (g_2^2 + h_2^2) e^{-2\alpha l} + C \cos 2r_1 + D \sin 2r_1} \quad (2)$$

where

$$g_1 = \frac{n_0^2 - n_1^2 - k_1^2}{(n_0 + n_1)^2 + k_1^2}$$

$$g_2 = \frac{n_1^2 - n_2^2 + k_1^2}{(n_1 + n_2)^2 + k_1^2}$$

$$h_1 = \frac{2n_0k_1}{(n_0 + n_1)^2 + k_1^2}$$

$$h_2 = \frac{-2n_2k_1}{(n_1 + n_2)^2 + k_1^2}$$

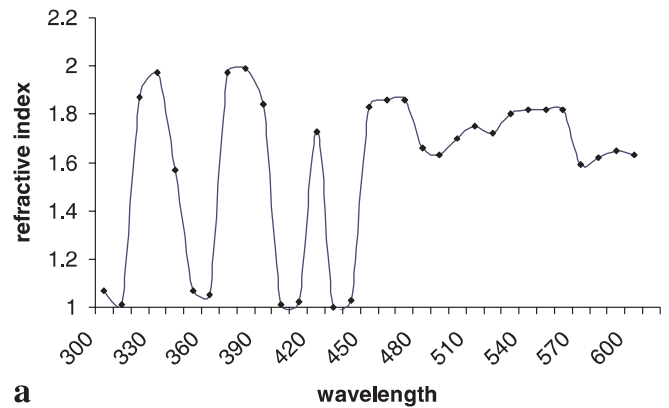
$$\alpha_1 = 2\pi kd/\lambda \quad r_1 = 2\pi n_1 d/\lambda$$

$$A = 2(g_1g_2 + h_1h_2), \quad B = 2(g_1h_2 - g_2h_1),$$

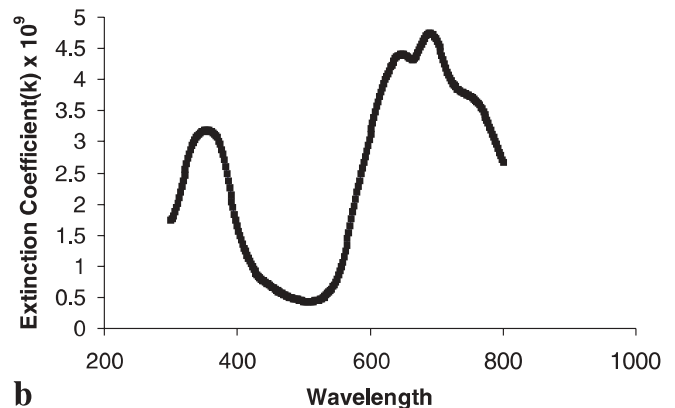
$$C = 2(g_1g_2 - h_1h_2), \quad D = 2(g_1h_2 + g_2h_1).$$

Here *d* is the thickness of the film, *l* is the wavelength of the incident radiation, *n*₀, *n*₁ and *n*₂ are the refractive indices of air, film and glass respectively and *k*₀, *k*₁ and *k*₂ are the extinction coefficients of air, film and glass respectively.

The values of *n* and *k* (real and imaginary parts of the complex refractive index) are determined from *R* and *T* using (1) and (2) by iteration. Iterations were carried out until the de-



a



b

FIGURE 11 Variation of a refractive index (*n*) and b extinction coefficient (*k*) with wavelength for a typical flash-evaporated ZnPc thin film

sired convergence was achieved. The absorption of radiation that gives rise to transition of electrons is generally given by the equation

$$\alpha^p = (A/h\gamma)(h\gamma - E_g).$$

The exponent p characterizes the type of transition and takes the values 2, 2/3, 1/2 and 1/3 for direct allowed, direct forbidden, indirect allowed and indirect forbidden transitions respectively. The absorption coefficient α can be determined from the transmittance spectrum using the well-known equation

$$\alpha = 1/d(A) \ln(T^{-1}),$$

where d is the film thickness and T is the transmittance of the sample.

The plot of α^2 versus phonon energy was plotted. From the plot, it is concluded that this material exhibits only the direct allowed transition. The variation of α^2 versus phonon energy for ZnPc thin films is shown in Fig. 10. From these absorption peaks, the direct and allowed band-gap energy of the Q band is evaluated as 1.97 eV. The variation of refractive index n and extinction coefficient k for ZnPc films is shown in Fig. 11 and no monotonic change is observed in either of them.

4 Conclusion

Zinc phthalocyanine in powder form exhibits a crystalline nature. Flash-evaporated ZnPc films exhibits an amorphous nature when deposited at room temperature (303 K substrate temperature), but their crystallinity increases with increase of the substrate temperature and more regular, crystalline films are obtained at higher substrate temperatures.

XRD analysis revealed the crystalline nature of the films. From the surface analysis using SEM and SPM it is revealed that there is a more homogeneous distribution of the particles and the surface is smooth and stoichiometric. From the thermal analysis it is observed that the phase change occurs at 538 K. From the optical analysis, it is found that the films possess a high absorption coefficient at the higher thicknesses. The optical transition in ZnPc films was found to be allowed and direct. The optical energy gap was found to be around 1.97 eV. The optical constants n and k were evaluated from the transmittance values. Since a ZnPc film exhibits a good absorption in the visible region of the electromagnetic spectrum, it can be good candidate for solar energy conversion devices. Hence it is concluded that, without sacrificing the homogeneity and the stoichiometry, ZnPc films can be deposited by the flash-evaporation method for various device applications.

ACKNOWLEDGEMENTS We would like to thank CONACYT (G386180U) for partial financial support.

REFERENCES

- 1 J. Ni, T. Tano, Y. Ichino, T. Hanada, T. Kamata, N. Takada, K. Yase: *Jpn. J. Appl. Phys.* **40**, L948 (2001)
- 2 N. Uyeda, M. Ashida, E. Suito: *J. Appl. Phys.* **36**, 1453 (1965)
- 3 P.A. Lane, J. Rostalski, C. Giebeler, S.J. Martin, D.D.C. Bradley, D. Meissner: *Sol. Energy Mater. Sol. Cells* **63**, 3 (2000)
- 4 D. Wrobel, A. Boguta: *J. Photochem. Photobiol. A: Chem.* **6045**, 1 (2002)
- 5 K. Oda, S.-I. Ogura, I. Okura: *J. Photochem. Photobiol. B: Biol.* **59**, 20 (2000)
- 6 M. Ashida, N. Uyeda, E. Suito: *Bull. Chem. Soc. Jpn.* **39**, 2616 (1966)
- 7 M.K. Debe, R.J. Poirier, K.K. Kam: *Thin Solid Films* **197**, 335 (1991)
- 8 M.J. Stillman, T. Nyokong: *Phthalocyanines, Properties and Applications*, ed. by C.C. Leznoff, A.B.P. Lever (VCD, New York 1989) Chapt. 3
- 9 D. Meissner, J. Rostalski: *Synthetic Metals* **121**, 1551 (2001)